*R*esearch in
*A*stronomy and
*A*strophysics

Structure of ADAFs in a general large-scale B-field: the role of wind and thermal conduction

Amin Mosallanezhad[1,2], Mehdi Khajavi[3] and Shahram Abbassi[2,4]

[1] Center for Excellence in Astronomy & Astrophysics (CEAA - RIAAM), P.O. Box 55134-441, Maragha, Iran
[2] School of Physics, Damghan University, P.O. Box 36715-364, Damghan, Iran
[3] Department of Physics, School of Sciences, Ferdowsi University of Mashhad, Mashhad, 91775-1436, Iran
[4] School of Astronomy, Institute for Research in Fundamental Sciences, P.O. Box 19395-5531, Tehran, Iran; *abbassi@ipm.ir*

Abstract We have explored the structure of a hot flow bathed in a general large-scale magnetic field. The importance of outflow and thermal conduction on the self-similar structure of a hot accretion flow has been investigated. We consider the additional magnetic parameters $\beta_{r,\varphi,z}\left[= c_{r,\varphi,z}^2/(2c_s^2)\right]$, where $c_{r,\varphi,z}^2$ are the Alfvén sound speeds in three directions of cylindrical coordinates. In comparison to the accretion disk without winds, our results show that the radial and rotational velocities of the disk become faster, but the disk becomes cooler because of the angular momentum and energy flux which are taken away by the winds. Moreover, thermal conduction opposes the effect of winds and not only decreases the rotational velocity but also increases the radial velocity as well as the sound speed of the disk. In addition, we study the effect of the global magnetic field on the structure of the disk. Our numerical results show that all the components of a magnetic field can be important and they have a considerable effect on velocities and vertical structure of the disk.

Key words: accretion: accretion flow — wind: outflow — thermal conduction

1 INTRODUCTION

Black hole accretion disks provide the most powerful energy-production mechanism in the universe. It is well accepted that many astrophysical systems are powered by black hole accretion. The standard thin disks (i.e., geometrically thin and optically thick accretion disks) can successfully explain most observational features of black hole accretion systems (Shakura & Sunyaev 1973). The ultraviolet/optical continuum emission observed in luminous quasars is usually attributed to thermal radiation from standard disks (SDs) surrounding massive black holes in quasars (e.g., Sun & Malkan 1989). However, the SD model is unable to reproduce the spectral energy distributions (SEDs) of many sources (e.g., Sgr A*) accreting at very low rates, and the advection dominated accretion flows (ADAFs) were suggested to be present in these sources (Narayan & Yi 1994, 1995). In the ADAF model, most gravitational energy in the gases is released in the accretion flow and is converted to the internal energy of the gas, making the ADAF hot, geometrically thick, and optically thin. Only

a small fraction of the released energy in ADAFs is radiated away, and their radiation efficiency is therefore significantly lower than that of standard thin disks (see Narayan et al. 1998 for a review and references therein, Kato et al. 2008).

There is also evidence that the process of mass accretion via a disk is often and perhaps always associated with mass loss from the disk in the form of a wind or a jet. Mass loss appears to be a common phenomenon among astrophysical accretion disk systems. These mass-loss mechanisms are observed in micro-quasars, young stellar objects and even brown dwarfs (Ferrari 1998; Bally et al. 2007; Whelan et al. 2005). An outflow emanating from an accretion disk can act as a sink for mass, angular momentum and energy and can therefore alter the dissipation rates and effective temperatures across the disk (Knigge 1999). The accretion flows lose their mass by winds as they flow on to the central object. As a result of mass loss, the accretion rate, $\dot{M}$, is no longer constant in terms of radius r. It is often expressed as $\dot{M} \propto r^s$ with s being a constant of order unity (Blandford & Begelman 1999).

Outflows have been found in numerical simulations of hot accretion flows that incorporate both hydrodynamic (HD) and magnetohydrodynamic (MHD) processes. The pioneering works that modeled outflows in HD simulations are by Igumenshchev & Abramowicz (1999, 2000) and Stone et al. (1999). Igumenshchev & Abramowicz (2000) have shown that convective accretion flows and flows with large-scale circulations have significant outward-directed energy fluxes, which have important implications for the spectra and luminosities of accreting black holes. The most recent work focusing on convective outflows is by Yuan & Bu (2010). As a result, they have shown that the mass accretion rate decreases inward, i.e., only a small fraction of the accretion gas can fall onto the black hole, while the rest circulates in the convective eddies or is lost in convective outflows. Stone & Pringle (2001), using MHD simulations, have reported the appearance of wind and outflow. In their simulations, the net mass accretion rate is small compared to the mass inflow and outflow rates at large radii associated with turbulent eddies.

Astrophysical jets and outflows emanating from accretion disks have been extensively investigated by many researchers. Various driving sources have been proposed, including thermal, radiative and magnetic ones. Traditionally, the name of the wind depends on its driving force. In this study we will follow the hydrodynamical (thermal) wind which has been discussed by many authors (see e.g. Meier 1979, 1982; Fukue 1989; Takahara et al. 1989).

The diversity of the models shows that modeling hot accretion flows is a challenging and controversial problem. One of the largely neglected physical phenomena in the modeling of ADAFs is thermal conduction. Recent observations of the hot accretion flows around active galactic nuclei indicated that that they operate in a collision-less regime (Tanaka & Menou 2006). Chandra observations provide tight constraints on the density and temperature of gas at or near the Bondi capture radius in Sgr A* and several other nearby galactic nuclei. Tanaka & Menou (2006) used these constraints (Loewenstein et al. 2001; Baganoff et al. 2003; Di Matteo et al. 2003; Ho et al. 2003) to calculate the mean free path for the observed gas. They have shown that accretion in these systems will proceed under the collision-less regime. They have suggested that thermal conduction could be a possible mechanism by which sufficient extra heating is provided in hot ADAFs. So, thermal conduction probably has an important role in energy transport of the accreting materials in a hot accretion disk where they are nearly completely ionized. The cooling dominated Shapiro, Lightman and Eardley (SLE) solution has been shown to be thermally unstable (Piran 1978; Wandel & Liang 1991; Narayan & Yi 1995) and, hence, is unlikely to exist in nature. It has been shown that any accretion flow in which the heating balances the cooling is thermally unstable, if the cooling is due to Bremsstrahlung emissions (Shakura & Sunyaev 1973; Piran 1978). However, an ADAF is known to be thermally stable (Narayan & Yi 1995; Kato et al. 1996, 1997) therefore the cooling is weak and the thermal energy of the flow is not radiated but advected with the gas. Since the advection-dominated disks have a high temperature, the internal energy per particle is high. This is one of the reasons why advective cooling overcomes radiative cooling. For the same reason, turbulent heat transport by

conduction in the radial direction is non-negligible in the heat balance equation. However, due to the very high temperature of the accreting gas, thermal conduction is very strong and could suppress the thermal instability. So it is important to consider the role of thermal conduction in an ADAF solution. Shadmehri (2008), Abbassi et al. (2008, 2010), Tanaka & Menou (2006), and Faghei (2012) have studied the effect of hot accretion flow with thermal conduction using a semi-analytical method; the dynamics of such systems have been studied in simulation models (e.g. Sharma et al. 2008; Wu et al. 2010). Shadmehri (2008) has shown that the thermal conduction opposes the rotational velocity, but increases the temperature. Abbassi et al. (2008) have shown that for these problems there are two types of solutions, high and low accretion rates. They plotted the radial velocity for both solutions which showed that it will be modified by thermal conduction.

Early work on disk accretion to a black hole argued that a large-scale magnetic field originating from the interstellar medium or even the central engine would be dragged inward and greatly compressed near the black hole by the accreting plasma (Bisnovatyi-Kogan & Ruzmaikin 1974, 1976). So, a large-scale B-field has an important role in the dynamics and structure of a hot accretion flow since the flow is highly ionized. The effect of a magnetic field on the structure of ADAFs were also studied (Balbus & hawley 1998; Kaburaki 2000; Shadmehri 2004; Meier 2005; Shadmehri & Khajenabi 2005, 2006; Ghanbari et al. 2007; Abbassi et al. 2008, 2010; Bu et al. 2009). Fukue & Akizuki (2006) and Abbassi et al. (2008) presented the self-similar solutions of the flow based on vertically integrated equations. However they have emphasized an intermediate case where the magnetic force is comparable to other forces by assuming the physical variables in the disk only act as a function of radius, and they merely discussed the global toroidal magnetic field in the disk. In reality, thermal conduction in a hot accretion flow should be anisotropic and along magnetic field lines. Anisotropic thermal conduction can induce magnetothermal instability (MTI) and significantly affects the dynamics of the hot accretion flow. Balbus (2001) has analytically proposed the existence of MTI. Later, MTI has been investigated using numerical simulations by Parrish & Stone (2005, 2007); Sharma et al. (2008); Bu et al. (2011).

In this paper, we first extend the work of Akizuki & Fukue (2006); Zhang & Dai (2008) and Abbassi et al. (2008, 2010) by considering a general large-scale magnetic field of all three components in cylindrical coordinates (r, φ, z) and then discuss the effects of the global magnetic field on the flows with thermal conduction and wind. We adopt the treatment that the flow variables are functions of the disk radius, and we neglect the different structure in the vertical direction except for the z-component in the momentum equation. We also compare our results with pervious studies, in which a large-scale magnetic field, thermal conduction and wind are neglected.

2 BASIC EQUATIONS

We are interested in analyzing the structure of a magnetized ADAF bathed in a global magnetic field where thermal conduction and wind play an important role in transportation of energy and angular momentum. So we suppose that the gaseous disk is rotating around a compact object of mass M_*. Thus, for a steady axi-symmetric accretion flow, i.e., $\partial/\partial t = \partial/\partial \varphi = 0$, we can write the standard equations in cylindrical coordinates (r, φ, z). We vertically integrate the flow equations, and all the physical variables become only a function of the radial distance r. We also neglect the relativistic effects, and Newtonian gravity in the radial direction is considered. Moreover, we consider a magnetic field in the disk with three components: B_r, B_φ and B_z.

The equation of continuity gives

$$\frac{\partial}{\partial r}(r \Sigma v_r) + \frac{1}{2\pi} \frac{\partial \dot{M}_{\mathrm{w}}}{\partial r} = 0, \tag{1}$$

where v_r is the radial infall velocity and Σ is the surface density at the cylindrical radius r, which is defined as $\Sigma = 2\rho H$, with ρ being the midplane density and H the half-thickness of the disk. In

addition, the mass loss rate by outflow/wind is represented by $\dot{M}_{\rm w}$, so

$$\dot{M}_{\rm w}(r) = \int 4\pi r' \dot{m}_{\rm w}(r')dr', \tag{2}$$

where $\dot{m}_{\rm w}(r)$ is the mass loss rate per unit area from each disk face. According to Blandford & Begelman (1999) and Shadmehri (2008), we can write the dependence of accretion rate as follows

$$\dot{M} = -2\pi r \Sigma v_r = \dot{M}_0 \Big(\frac{r}{r_0}\Big)^s, \tag{3}$$

where $\dot{M}_0$ is the mass accretion rate of the disk material at the outer region of the disk r_0 and s is a constant of order unity (Blandford & Begelman 1999). For a disk with outflow/wind, $s > 0$ while in the absence of wind/outflow, we consider $s = 0$ (Fukue 2004).

By considering Equations (1)–(3), we can have

$$\dot{m}_{\rm w} = s \frac{\dot{M}_0}{4\pi r_0^2} \Big(\frac{r}{r_0}\Big)^{s-2}. \tag{4}$$

The equation of motion in the radial direction is

$$v_r \frac{dv_r}{dr} = \frac{v_\varphi^2}{r} - \frac{GM_*}{r^2} - \frac{1}{\Sigma}\frac{d}{dr}(\Sigma c_{\rm s}^2) - \frac{1}{2\Sigma}\frac{d}{dr}(\Sigma c_\varphi^2 + \Sigma c_z^2) - \frac{c_\varphi^2}{r}, \tag{5}$$

where v_φ is the rotational velocity, $c_{\rm s}$ the isothermal sound speed, which is defined as $c_{\rm s}^2 \equiv p_{\rm gas}/\rho$, and $p_{\rm gas}$ being the gas pressure. Also, c_r, c_φ and c_z are Alfvén sound speeds in three directions of cylindrical coordinates and are defined as $c_{r,\varphi,z}^2 \equiv B_{r,\varphi,z}^2/(4\pi\rho)$.

We assume that only the φ-component of the viscous stress tensor is important which is $t_{r\varphi} = \mu r d\Omega/dr$, where $\mu(\equiv \nu\rho)$ is the viscosity and ν is the kinematic coefficient of viscosity. We assume

$$\nu = \alpha c_{\rm s} H. \tag{6}$$

Here α is the standard viscosity parameter which is constant and less than unity (Shakura & Sunyaev 1973).

The angular transfer equation considering outflow/wind can be written as

$$\frac{v_r}{r}\frac{d}{dr}(rv_\varphi) = \frac{1}{r^2\Sigma}\frac{d}{dr}\Big(\nu\Sigma r^3\frac{d\Omega}{dr}\Big) + \frac{c_r}{\sqrt{\Sigma}}\frac{d}{dr}(\sqrt{\Sigma}c_\varphi) + \frac{c_r c_\varphi}{r} - \frac{l^2\Omega}{2\pi\Sigma}\frac{d\dot{M}_{\rm w}}{dr}, \tag{7}$$

where the last term on the right side represents angular momentum carried by the outflowing material. Here $l = 0$ corresponds to a non-rotating wind and $l = 1$ to outflowing material that carries away the specific angular momentum (see e.g., Knigge 1999).

Similarly, by integrating over z of the hydrostatic balance, we will have

$$\Omega_K^2 H^2 - \frac{1}{\sqrt{\Sigma}}c_r \frac{d}{dr}(\sqrt{\Sigma}c_z)H = c_{\rm s}^2 + \frac{1}{2}(c_r^2 + c_\varphi^2). \tag{8}$$

Now we can write the energy equation considering cooling and heating processes in ADAFs. We assume the generation of energy due to viscous dissipation and heat conduction into the volume are balanced by the advection cooling and energy loss of the outflow. Thus

$$\frac{\Sigma v_r}{\gamma - 1}\frac{dc_{\rm s}^2}{dr} - 2Hv_r c_{\rm s}^2\frac{d\rho}{dr} = f\nu\Sigma r^2\Big(\frac{d\Omega}{dr}\Big)^2 - \frac{2H}{r}\frac{d}{dr}(rF_{\rm s}) - \frac{1}{2}\eta\dot{m}_{\rm w}(r)v_K^2(r), \tag{9}$$

where the second term on the right hand side represents the energy transfer due to the thermal conduction and $F_\mathrm{s}(= 5\phi_\mathrm{s}\rho c_\mathrm{s}^3)$ is the saturated conduction flux (Cowie & McKee 1977). The dimensionless coefficient ϕ_s is less than unity. Also, the last term on the right hand side of the energy equation is the energy loss due to wind or outflow (Knigge 1999). Depending on the energy loss mechanism, the dimensionless parameter η may change. In our case, we consider it as a free parameter (Knigge 1999).

To measure the magnetic field escaping/creating rate, we can write the three components of the induction equation, $(\dot{B}_r, \dot{B}_\varphi, \dot{B}_z)$, as

$$\dot{B}_r = 0, \tag{10}$$

$$\dot{B}_\varphi = \frac{d}{dr}(v_\varphi B_r - v_r B_\varphi), \tag{11}$$

$$\dot{B}_z = -\frac{d}{dr}(v_r B_z) - \frac{v_r B_z}{r}, \tag{12}$$

where $\dot{B}_{r,\varphi,z}$ is the field escaping/creating rate due to magnetic instability or the dynamo effect. Here we have a set of MHD equations that describe the structure of magnetized ADAFs. The solutions to these equations are strongly correlated to viscosity, magnetic field strength $\beta_{r,\varphi,z}$, the degree of advection f, wind parameter s and the thermal conduction parameter ϕ_s for the disks. We will seek a self-similar solution for the above equations in the next section.

3 SELF-SIMILAR SOLUTIONS

In order to have a better understanding of the physical processes taking place in our disks, we seek self-similar solutions of the above equations. The self-similar method has a wide range of applications for the full set of MHD equations, although it is unable to describe the global behavior of accretion flows since no boundary conditions have been taken into account. However, as long as we are not interested in the behavior of the flow near the boundaries, these solutions are still valid.

We assume that the physical quantities can be expressed as a power law of radial distance, i.e., r^ν, where ν is determined by substituting the similarity solutions into the main equations and solving the resulting algebraic equations. Therefore, we can write similarity solutions as

$$\Sigma(r) = c_0 \Sigma_0 \left(\frac{r}{r_0}\right)^{s-\frac{1}{2}}, \tag{13}$$

$$v_r(r) = -c_1 \sqrt{\frac{GM_*}{r_0}} \left(\frac{r}{r_0}\right)^{-\frac{1}{2}}, \tag{14}$$

$$v_\varphi(r) = c_2 \sqrt{\frac{GM_*}{r_0}} \left(\frac{r}{r_0}\right)^{-\frac{1}{2}}, \tag{15}$$

$$c_\mathrm{s}^2(r) = c_3 \left(\frac{GM_*}{r_0}\right) \left(\frac{r}{r_0}\right)^{-1}, \tag{16}$$

$$c_{r,\varphi,z}^2(r) = \frac{B_{r,\varphi,z}^2}{4\pi\rho} = 2\beta_{r,\varphi,z} c_3 \left(\frac{GM_*}{r_0}\right) \left(\frac{r}{r_0}\right)^{-1}, \tag{17}$$

$$H(r) = c_4 r_0 \left(\frac{r}{r_0}\right), \tag{18}$$

where constants c_0, c_1, c_2, c_3 and c_4 will be determined later from the main MHD equation. Σ_0 and r_0 are exploited to write the equations in non-dimensional forms and the constants $\beta_{r,\varphi,z}$ measure the ratio of the magnetic pressure in three directions to the gas pressure, i.e., $\beta_{r,\varphi,z} = p_{\mathrm{mag},r,\varphi,z}/p_\mathrm{gas}$.

In addition, the field escaping/creating rate $\dot{B}_{r,\varphi,z}$ is assumed to be in the form

$$\dot{B}_{r,\varphi,z} = \dot{B}_{r0,\varphi0,z0}\left(\frac{r}{r_0}\right)^{\frac{1}{2}\left(s-\frac{11}{2}\right)}, \tag{19}$$

where $\dot{B}_{r0,\varphi0,z0}$ is constant.

By substituting the above self-similar solutions in the continuity, momentum, angular momentum, hydrostatic balance and energy equation of the disk, we obtain the following system of dimensionless equations to be solved for c_0, c_1, c_2 c_3 and c_4:

$$c_0 c_1 = \dot{m}, \tag{20}$$

$$-\frac{1}{2}c_1^2 = c_2^2 - 1 - \left[\left(s - \frac{3}{2}\right) + \left(s - \frac{3}{2}\right)\beta_z + \left(s + \frac{1}{2}\right)\beta_\varphi\right]c_3, \tag{21}$$

$$-\frac{1}{2}c_1 c_2 = -\frac{3}{2}\left(s + \frac{1}{2}\right)\alpha c_2 \sqrt{c_3}c_4 + \left(s + \frac{1}{2}\right)c_3\sqrt{\beta_r \beta_\varphi} - sl^2\frac{\dot{m}}{c_0}c_2, \tag{22}$$

$$c_4 = \frac{1}{2}\left[\sqrt{\left(s - \frac{3}{2}\right)^2 \beta_r \beta_z c_3^2 + 4(1 + \beta_r + \beta_\varphi)c_3} + \left(s - \frac{3}{2}\right)\sqrt{\beta_r \beta_z}c_3\right], \tag{23}$$

$$\left(\frac{1}{\gamma - 1} + s - \frac{3}{2}\right)c_1 c_3 = \frac{9}{4}\alpha f c_2^2 \sqrt{c_3}c_4 - 5\phi_s(s - 2)c_3^{\frac{3}{2}} - \frac{s}{4}\eta\frac{\dot{m}}{c_0}, \tag{24}$$

where $\dot{m}$ is the non-dimensional mass accretion rate which is defined as

$$\dot{m} = \frac{\dot{M}_0}{2\pi r_0 \Sigma_0 \sqrt{GM_*/r_0}}. \tag{25}$$

If we solve the self-similar structure of the magnetic field escaping rate, we will have:

$$\dot{B}_{0r} = 0, \tag{26}$$

$$\dot{B}_{0\varphi} = \frac{1}{2}\left(s - \frac{7}{2}\right)\frac{GM_*}{r_0^{5/2}}\sqrt{\frac{4\pi c_0 c_3 \Sigma_0}{c_4}} \times \left(c_2\sqrt{\beta_r} + c_1\sqrt{\beta_\varphi}\right), \tag{27}$$

$$\dot{B}_{0z} = \frac{1}{2}\left(s - \frac{3}{2}\right)c_1\frac{GM_*}{r_0^{5/2}}\sqrt{\frac{4\pi\beta_z c_0 c_3 \Sigma_0}{c_4}}. \tag{28}$$

We can solve these simple equations numerically and clearly so the physical solution can be interpreted. Without the mass outflow, thermal conduction and magnetic field, i.e. $s = l = \eta = \phi_s = \beta_r = \beta_\varphi = \beta_z = 0$, the equations and their similarity solutions are reduced to the standard ADAF solution (Narayan & Yi 1994). Also, in the absence of outflow and thermal conduction they are reduced to Zhang & Dai (2008).

Now we can analyze behavior of the solutions in the presence of wind, thermal conduction and a global magnetic field. The parameters of our model are the standard viscosity parameter α, advection parameter f, ratio of the specific heats γ, the mass-loss parameter s, degree of magnetic pressure to gas pressure in three dimensions of cylindrical coordinates, β_r, β_φ and β_z, the saturated conduction parameter ϕ_s and l, η parameters corresponding to wind/outflows.

Four panels in Figure 1 show the variations of coefficients c_0, c_1, c_2 and c_3 in terms of the wind parameter s for different values of the thermal conduction parameter ϕ_s, i.e., $\phi_s = 0.001$ (dotted line), $\phi_s = 0.01$ (dashed line) and $\phi_s = 0.02$ (solid line), corresponding to $\alpha = 0.2$, $\gamma = 4/3$, $\beta_r = \beta_\varphi = \beta_z = 1.0$, $\eta = l = 0.1$ and $f = 1.0$ (full advection).

In the upper-left panel of Figure 1 we can see that for a non-zero s, the surface density is lower than the standard ADAF solution, and for stronger outflows, the reduction of the surface density is

more evident. Also, the surface density decreases by increasing the thermal conduction. The upper-right panel of Figure 1 represents the behavior of the radial infall velocity compared to the Keplerian one. Although the radial velocity is slower than the Keplerian velocity, it becomes faster by increasing f and α. We know that the value of s measures the strength of the outflow/wind, and large values of s denote a strong wind/outflow. So we can see that the radial flows of the accreted materials become larger by increasing the wind parameter s. Moreover, thermal conduction increases the radial infall velocity.

It is clear from the bottom panels of Figure 1 that the rotational velocity increases when the wind parameter s is added. Although thermal conduction decreases the rotational speed, it is shown that temperature decreases for strong outflows (bottom-right panel). On the other hand, the outflow/wind acts as a cooling agent (Shadmehri 2008; Abbassi et al. 2010).

Figure 2 shows how the coefficients c_i depend on the magnetic parameter in the radial direction β_r for several values of the outflow parameter s. We can see that the surface density becomes larger if the wind parameter $s(0-0.3)$ increases. It is obvious that $s = 0$ represents solutions where no wind is present (Tanaka & Menou 2006). By adding β_r, we see that the surface density and sound speed decrease while the radial and rotational velocity increase. This is the same as in Figure 1, where the outflow increases the radial and rotational velocity, although the sound speed and surface density decrease when the wind parameter increases.

In Figure 3, behaviors of the coefficients c_i versus toroidal magnetic field B_φ (β_φ) are shown for different values of s. From the upper-left panels of Figure 3, we can see that for $\beta_\varphi (= 0-5)$, the radial infall velocity is sub-Keplerian, and that it becomes larger by increasing the wind parameter s. In addition, when the toroidal magnetic field becomes stronger, the radial velocity of the accretion materials increases. This is due to the magnetic tension terms, which dominate the magnetic pressure term in the radial momentum equation that assists the radial infall motion. The bottom-right panel in Figure 3 displays the rotational velocity of the accretion disk. We see that for the given advection parameter $f(= 1.0)$ and $\beta_r = \beta_z = 1.0$, the rotational velocity increases as the toroidal magnetic field becomes stronger. The crucial point is that when the toroidal magnetic field is very strong, the rotational velocity will be super-Keplerian (i.e., $\beta_\varphi \sim 5$). Moreover, the surface density of the disk decreases when the toroidal magnetic field becomes too large.

In Figure 3, the isothermal sound speed of the disk has distinctive properties between $\beta_\varphi < 1$ and $\beta_\varphi > 1$. When β_φ is below unity, the isothermal sound speed decreases, although for $\beta_\varphi > 0$, it increases. This means that there is a minimum near $\beta_\varphi \sim 1$, because the parameters $\beta_r = \beta_z (= 1.0)$ are present in our calculation and both of them decrease the isothermal sound speed. So when the toroidal magnetic field dominates, the sound speed starts to become larger.

In Figure 4 we have plotted the coefficients c_i with the z-component of the magnetic field for different values of s. We first find that a strong z-component of the magnetic field (β_z) leads to a decrease in the infall velocity v_r, rotational velocity v_φ and isothermal sound speed c_s of the disk, which means that a strong magnetic pressure in the vertical direction prevents the disk matter from being accreted, and decreases the effect of gas pressure as the accretion proceeds. However, the surface density of the disk increases by increasing the z-component of the magnetic field.

4 GENERAL PROPERTIES OF ACCRETION FLOWS

In the previous section we have introduced self-similar solutions and their properties for an ADAF bathed in a large-scale B-field with thermal conduction and outflow. Having this self-similar solution allows us to investigate the general properties of the disk, so we can see how thermal conduction and wind will affect the physical quantities of the disks.

The mass-accretion rate in the disk can be written by a simple lapse function of radius due to the effect of outflow and thermal conduction. Using the self-similar solution we can estimate the mass
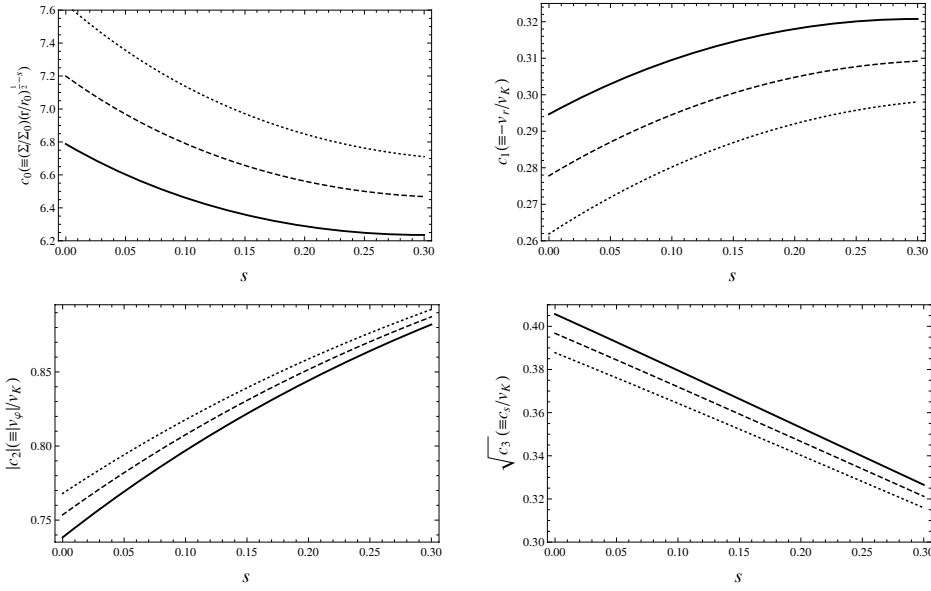
Fig. 1 Numerical coefficients c_i as a function of the wind parameter s for several values of the thermal conduction parameter ϕ_s. The dotted, dashed and solid lines correspond to $\phi_s = 0.001, 0.01$ and 0.02 respectively. Parameters are set as $\alpha = 0.2$, $\gamma = 4/3$, $\beta_r = \beta_\varphi = \beta_z = 1.0$, $\eta = l = 0.1$ and $f = 1$.
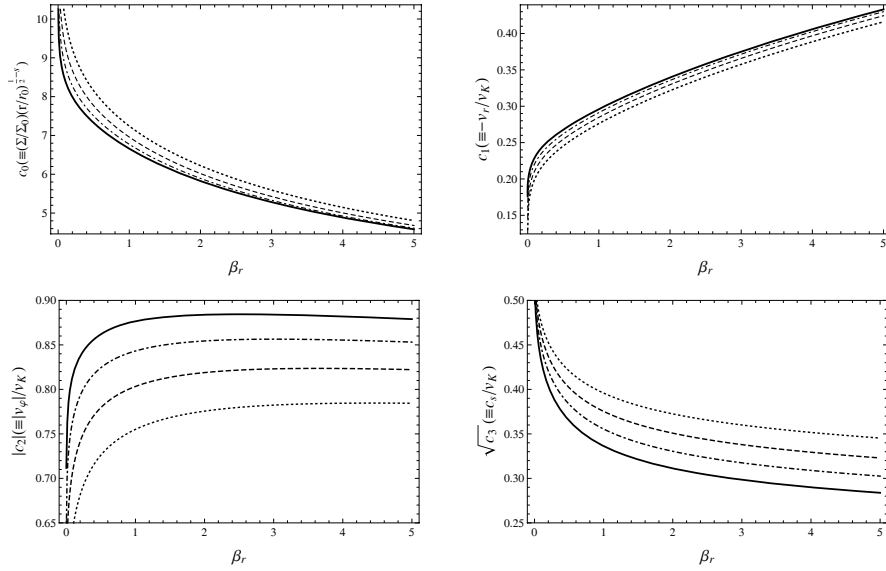

Fig. 2 Numerical coefficients c_i as a function of the magnetic parameter β_r for several values of the wind parameter s. The dotted, dashed, dash-dotted and solid lines correspond to $s = 0.0, 0.1, 0.2$ and 0.3 respectively. Parameters are set as $\alpha = 0.2$, $\gamma = 4/3$, $\beta_\varphi = \beta_z = 1.0$, $\phi_s = 0.01$, $\eta = l = 0.1$ and $f = 1$.
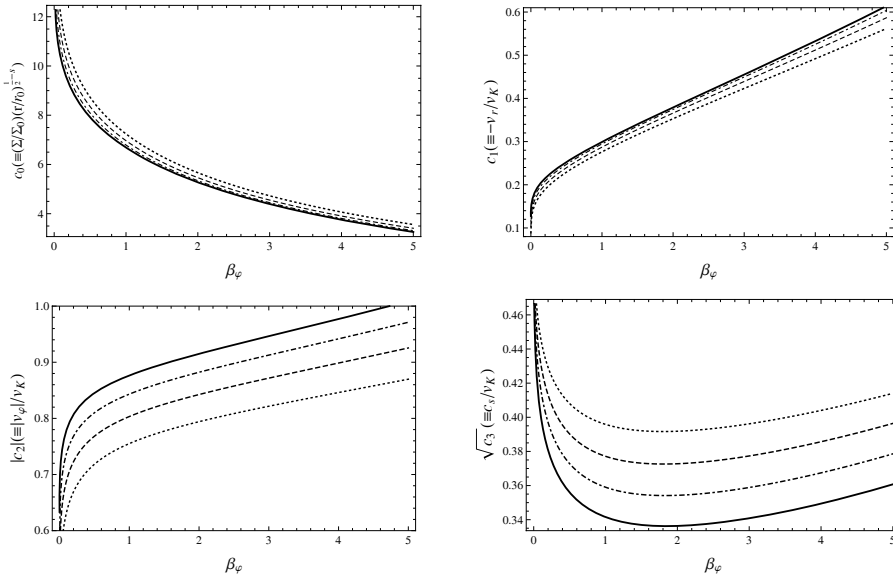
Fig. 3 Numerical coefficients c_i as a function of magnetic parameter β_φ for several values of s. The dotted, dashed, dash-dotted and solid lines correspond to $s = 0.0, 0.1, 0.2$ and 0.3 respectively. Parameters are set as $\alpha = 0.2$, $\gamma = 4/3$, $\beta_r = \beta_z = 1.0$, $\phi_s = 0.01$, $\eta = l = 0.1$ and $f = 1$.
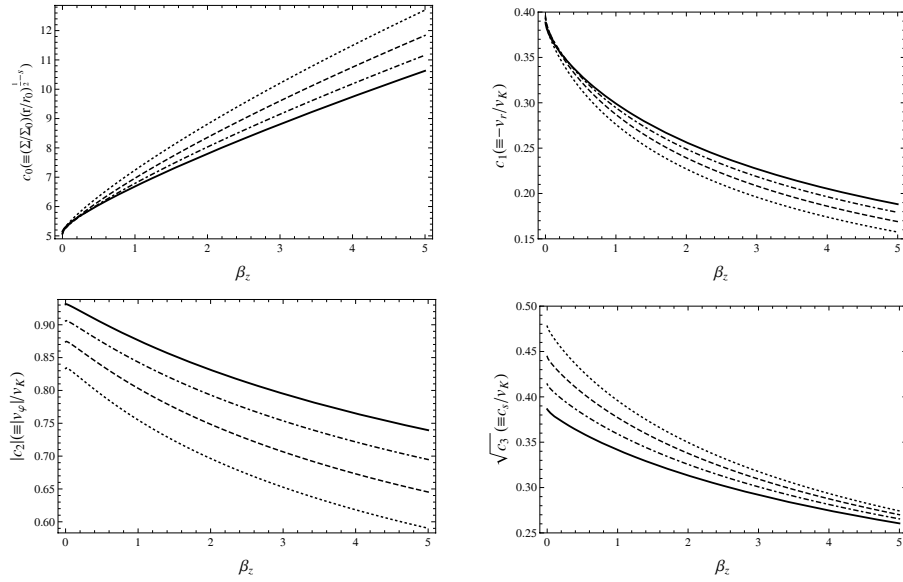

Fig. 4 Numerical coefficients c_i as a function of the magnetic parameter β_z for several values of s. The dotted, dashed, dash-dotted and solid lines correspond to $s = 0.0, 0.1, 0.2$ and 0.3 respectively. Parameters are set as $\alpha = 0.2$, $\gamma = 4/3$, $\beta_r = \beta_\varphi = 1.0$, $\phi_s = 0.01$, $\eta = l = 0.1$ and $f = 1$.

accretion rate as

$$\dot{M} = -2\pi r \Sigma v_r = 2\pi c_0 c_1 \Sigma_0 \left(\frac{GM_*}{r_0}\right)^{\frac{1}{2}} \left(\frac{r}{r_0}\right)^s = \dot{M}_{\text{out}} \left(\frac{r}{r_{\text{out}}}\right)^s, \tag{29}$$

where r_{out} and $\dot{M}_{\text{out}}$ are the outer radius and accretion rate respectively. As in the last section, thermal conduction, wind and the large scale B-field will affect c_0 and c_1 through their parameters s, ϕ and $\beta_{r,\phi,z}$. In the case of an accretion disk with no wind, $s = 0$, the accretion rate is independent of the radius, but for those with wind, $s > 0$, the accretion rate decreases with radius as we expect. Because winds start from various radii, the mass-loss rate is not constant but rather depends on the radius. As a result, some of the accreted materials are not concentrated at the center, but are diluted over a wide space. According to the mass loss from wind, the accretion rate decreases with radius as we expect.

If the central star is a black hole of mass M, it will grow via accretion. We can simply estimate the growth rate of the black hole using the accretion rate, which is also be implicitly affected by wind, thermal conduction and the large-scale B-field.

We can show the radial behavior of temperature of the self-similar ADAF disks with a large-scale magnetic field, thermal conduction and outflow. Optical depths of accretion flows are highly dependent on their accretion rate. These ADAFs occur in two regimes depending on their mass accretion rate and optical depth. In a high mass accretion rate, the optical depth becomes very high and the radiation generated by accretion flows can be trapped within the disk. This type of accretion disk is known as an optically thick or slim disk. In the limit of the low mass-accretion rates, the disk becomes optically thin. In this case, the cooling time of the accretion flow is longer than the accretion's timescale. The energy generated by accretion flows therefore mostly remains in the disks and the disks cannot radiate their energy efficiently. So, we should expect that the large scale B-field will implicitly affect the optical depth and accretion rate through the coefficients c_0 and c_1.

It should be emphasized that the radiative properties of optically thin disks, such as L_ν, cannot be calculated easily. In this case, the importance of advective cooling in optically thin disks should be demonstrated. In order to clarify this problem we should show how cooling and heating change with r, f and $\dot{M}$. Radiative cooling generally has very complicated parameter dependencies. In the optically thin cases, emission from the gas is not a black body continuum. Bremsstrahlung cooling in non-relativistic or relativistic cases, as well as synchrotron and Compton cooling may have possible roles in generating emission spectra.

In the optically thick case that we are trying to study, the radiation pressure dominates and sound speed is related to the radiation pressure. We can write the average flux F as

$$F = \sigma T_c^4 = \frac{3c}{8H}\Pi_{\text{gas}} = \frac{3c}{8}\Sigma_0 \frac{c_0 c_3}{c_4}\left(\frac{GM_*}{r_0^2}\right)\left(\frac{r}{r_0}\right)^{s-\frac{5}{2}}, \tag{30}$$

where $\Pi_{\text{gas}} = \Sigma c_s^2$ is the height-integrated gas pressure, T_c the disk's central temperature and σ the Stefan-Boltzmann constant. For the optically thick case, the optical thickness of the disk in the vertical direction is

$$\tau = \frac{1}{2}\kappa\Sigma = \frac{1}{2}\Sigma_0 c_0 \left(\frac{r}{r_0}\right)^{s-\frac{1}{2}}, \tag{31}$$

where κ is the opacity of electron scattering. We can thus calculate the effective flux and effective temperature of the disk surface as

$$F_{\text{eff}} = \sigma T_{\text{eff}}^4 = \frac{\sigma T_c^4}{\tau} = \left(\frac{3}{16\pi\sigma}\frac{c_3}{c_4}L_E\right)^{\frac{1}{4}} r^{-\frac{1}{2}}, \tag{32}$$

where $L_{\mathrm{E}} = 4\pi c \frac{GM}{\kappa}$ is the Eddington luminosity of the central object. If we integrate these equations radially, we obtain the disk luminosity as

$$L_{\mathrm{disk}} = \int_{r_{\mathrm{in}}}^{r_{\mathrm{out}}} 2\sigma T_{\mathrm{eff}}^4 2\pi r dr = \frac{3}{4} L_{\mathrm{E}} \frac{c_3}{c_4} \ln\left(\frac{r_{\mathrm{out}}}{r_{\mathrm{in}}}\right). \tag{33}$$

It should be emphasized that the luminosity and effective temperature of the disk are not affected by the mass-loss through outflow, magnetic field or thermal conduction (there are no s, $\beta_{r,\phi,z}$ or ϕ_s dependencies). However, wind would implicitly affect the radiative appearance of the disk through c_3 and c_4 in these formulae. The average flux decreases all over the disk when we have mass loss through outflow compared with the case of no mass loss. The surface density and therefore optical depth decrease for the case of mass loss. Hence, we can see the deep inner region of the disk.

5 CONCLUSIONS

In this paper, we studied an accretion disk in the advection dominated regime by considering a global magnetic field in the presence of wind and thermal conduction. Some approximations were made in order to simplify the main equations. We assumed an axially symmetric, static disk with the α-prescription of viscosity, $\nu = \alpha c_s H$. A set of similarity solutions was presented for such a configuration. We have extended the Akizuki & Fukue (2006); Zhang & Dai (2008) and Abbassi et al. (2010) self similar solutions to present a dynamic structure of the ADAFs. We ignored the relativistic effects and the self-gravity of the disks. Considering the weakly colliding nature of a hot accretion flow (Tanaka & Menou 2006; Abbassi et al. 2008), a saturated form of thermal conduction was adopted as a possible mechanism for energy transportation. We have accounted for this possibility by allowing the saturated thermal conduction constant, ϕ_s, to vary in our solutions.

We have shown that a strong wind could have a lower temperature which fits with the results that were presented by Kawabata & Mineshige (2009), which could make a significant difference in the observed flux compared to standard ADAFs. The most important finding of our simple self-similar solution is that the accreted flow is strongly affected not only by mass loss but also by energy loss of the wind. However, some limitations to our solutions exist. One is that the self-similar hot accretion flow with conduction is a single-temperature structure. Thus if one uses a two-temperature structure for the ions and electrons in the disks, it is expected that the ions and electron temperatures will decouple in the inner regions, which will modify the role of conduction. The other limitation of our solution is the anisotropic character of conduction in the presence of a magnetic field. Balbus (2001) has argued that the structure of the hot flows could be affected by the anisotropic character of thermal conduction in the presence of a magnetic field.

Although our preliminary self-similar solutions are quite simplified, they clearly improve our understanding of the physics of ADAFs around a black hole. To have a realistic picture of an accretion flow, a global solution is needed rather than a self-similar one. In future studies we intend to investigate the effect of thermal conduction on the observational appearance and properties of a hot magnetized flow.

References

Abbassi, S., Ghanbari, J., & Najjar, S. 2008, MNRAS, 388, 663

Abbassi, S., Ghanbari, J., & Ghasemnezhad, M. 2010, MNRAS, 409, 1113

Akizuki, C., & Fukue, J. 2006, PASJ, 58, 469

Baganoff F. K., Maeda Y., Morris M., et al. 2003, ApJ, 591, 891

Balbus, S. A. 2001, ApJ, 562, 909

Balbus, S., & Hawley, J. F. 1998, RvMP, 70, 1

Bally, J., Reipurth, B., & Davis, C. J. 2007, Protostars and Planets V (University Arizona press), 215

Bisnovatyi-Kogan, G. S., & Ruzmaikin, A. A. 1974, Ap&SS, 28, 31

Bisnovatyi-Kogan, G. S., & Ruzmaikin, A. A. 1976, Ap&SS, 42, 401

Blandford, R. D., & Begelman, M. C. 1999, MNRAS, 303, L1

Bu, D.-F., Yuan, F., & Xie, F.-G. 2009, MNRAS, 392, 325

Bu, D.-F., Yuan, F., & Stone, J. M. 2011, MNRAS, 413, 2808

Cowie, L. L., & McKee, C. F. 1977, ApJ, 211, 135

Di Matteo, T., Allen, S. W., Fabian, A. C., Wilson, A. S., & Young, A. J. 2003, ApJ, 582, 133

Faghei, K. 2012, Ap&SS, 338, 301

Ferrari, A. 1998, ARA&A, 36, 539

Fukue, J. 1989, PASJ, 41, 123

Fukue, J. 2004, PASJ, 56, 181

Fukue, J., & Akizuki, C. 2006, PASJ, 58, 1073

Ghanbari, J., Salehi, F., & Abbassi, S. 2007, MNRAS, 381, 159

Ho, L. C., Terashima, Y., & Ulvestad, J. S. 2003, ApJ, 589, 783

Igumenshchev, I. V., & Abramowicz, M. A. 1999, MNRAS, 303, 309

Igumenshchev, I. V., & Abramowicz, M. A. 2000, ApJS, 130, 463

aburaki, O. 2000, ApJ, 531, 210

Kato, S., Abramowicz, M. A., & Chen, X. 1996, PASJ, 48, 67

Kato, S., Yamasaki, T., Abramowicz, M. A., & Chen, X. 1997, PASJ, 49, 221

Kato, S., Fukue, J., & Mineshige, S. 2008, Black-Hole Accretion Disks — Towards a New Paradigm (Kyoto
    Univ. Press)

Kawabata, R., & Mineshige, S. 2009, PASJ, 61, 1135

Knigge, C. 1999, MNRAS, 309, 409

Loewenstein, M., Mushotzky, R. F., Angelini, L., Arnaud, K. A., & Quataert, E. 2001, ApJ, 555, L21

Meier, D. L. 1979, ApJ, 233, 664

Meier, D. L. 1982, ApJ, 256, 706

Meier, D. L. 2005, Ap&SS, 300, 55

Narayan, R., Mahadevan, R., & Quataert, E. 1998, in Theory of Black Hole Accretion Disks, eds. M. A.
    Abramowicz, G. Bjornsson, & J. E. Pringle (Cambridge Univ. Press), 148

Narayan, R., & Yi, I. 1994, ApJ, 428, L13

Narayan, R., & Yi, I. 1995, ApJ, 444, 231

Parrish, I. J., & Stone, J. M. 2005, ApJ, 633, 334

Parrish, I. J., & Stone, J. M. 2007, ApJ, 664, 135

Piran, T. 1978, ApJ, 221, 652

Shadmehri, M. 2004, A&A, 424, 379

Shadmehri, M. 2008, Ap&SS, 317, 201

Shadmehri, M., & Khajenabi, F. 2005, MNRAS, 361, 719

Shadmehri, M., & Khajenabi, F. 2006, ApJ, 637, 439

Shakura, N. I., & Sunyaev, R. A. 1973, A&A, 24, 337

Sharma, P., Quataert, E., & Stone, J. M. 2008, MNRAS, 389, 1815

Sun, W.-H., & Malkan, M. A. 1989, ApJ, 346, 68

Stone, J. M., & Pringle, J. E. 2001, MNRAS, 322, 461

Stone, J. M., Pringle, J. E., & Begelman, M. C. 1999, MNRAS, 310, 1002

Takahara, F., Rosner, R., & Kusunose, M. 1989, ApJ, 346, 122

Tanaka, T., & Menou, K. 2006, ApJ, 649, 345

Wandel, A., & Liang, E. P. 1991, ApJ, 380, 84

Whelan, E. T., Ray, T. P., Bacciotti, F., et al. 2005, Nature, 435, 652

Wu, M., Yuan, F., & Bu, D. 2010, Science in China G: Physics and Astronomy, 53, 168

Yuan, F., & Bu, D.-F. 2010, MNRAS, 408, 1051

Zhang, D., & Dai, Z. G. 2008, MNRAS, 388, 1409